International Journal of Electrical and Computer Engineering (IJECE)
Vol. 10, No. 3, June 2020, pp. 3323~3332
ISSN: 2088-8708, DOI: 10.11591/ijece.v10i3.pp3323-3332

Improved magnetic behavior of hemicycle PM motor via stator modification

Kwang T. C., Mohd Luqman Mohd Jamil, Auzani Jidin
Power Electronics and Drive Research Group (PEDG), Universiti Teknikal Malaysia Melaka, Malaysia

Article Info

Article history:

Received Sep 26, 2019
Revised Dec 9, 2019
Accepted Jan 31, 2020

Keywords:

Hemicycle stator
PM motor
Weight reduction

ABSTRACT

This article investigates electromagnetic performance of a hemicycle PM motor by introducing a little modification on both ends of a hemicycle stator. Prior to the investigation, an analytical model for the hemicycle PM motor weight is derived analytically for the purpose of comparison with a conventional design. Both motor weights are then verified and the hemicycle motor is found to have lighter weight than the conventional design. By having a proper design modification, an optimum motor performance is achievable due to improved magnetic permeance. Two designs that have different arc angle; i) 180° (188.5 mm arc length) and ii) >180° (204.2 mm arc length) are the subjects of investigation. It is found that a hemicycle PM motor in which arc angle >180° results maximum torque average with the smallest torque ripple and smallest cogging torque.

Corresponding Author:

Mohd Luqman Bin Mohd Jamil,
Power Electronics and Drives Research Group (PEDG)
Universiti Teknikal Malaysia Melaka,
Hang Tuah Jaya, 76100 Durian Tunggal, Melaka, Malaysia
Email: luqman@utem.edu.my

1. INTRODUCTION

According to National Electrical Manufacturers Associations (NEMA), Permanent Magnet (PM) motors are electronically commutated and required three phase inverters for a desired rotation [1]. Due to high torque density, high efficiency, reliability and lightweight structure, PM motors become a favourable choice in high-torque low-speed applications compared to Brushed DC motors and Stepper motors [2-6]. Recently, electric machines benefit mankind in handling variation specific tasks due to limited human capability. However, some designs i.e. radial flux orientation machines were inherently came out with bulky size, low torque density, low efficiency and consumed high input power for dedicated applications. In [7, 8], investigations on axial flux oriented design that focused on drive train capability and parametric components were conducted to overcome these issues. A comparative study between single-sided and dual-sided, radial and axial flux orientation motors is presented to justify the pros and cons between these motors topologies. Figure 1 shows a general overview of PM motor topologies that are possible to achieve high-torque low-speed or low-torque high-speed performances.

Radial-flux PM motors configured with single-side design, slotted or slotless are made up of stacked steel laminations and copper coil wound around stator teeth. By having a proper sizing of stator slots, slotted configuration resulted high electric loading, high torque density, high efficiency, high output average torque as well as workable cost as compared to the slotless type [9-10]. However, high cogging torque, a rise in acoustic noise and vibration is inevitable. Variations of stator design such as non-slotted, skewing, dummy slots, notch slots and fractional slot configuration are beneficial for cogging torque and torque ripple minimizations [11]. Recently, high output torque and high power density in radial flux orientated motors are

essential to achieve an optimum performance. In this case, double-sided of Radial Flux Permanet magnet Motor (RFPM) is preferable where the motors are configured with dual-rotor and single-stator or dual-stator and single-rotor individually. For dual rotor topology, two sets of permanent magnets were mounted on different surfaces, at the outer stator and inner stator surfaces respectively. This configuration resulted lower usage of copper winding leading to a relative high of motor's efficiency and its torque density as compared to the conventional design [12, 13]. Yet, more complex structure, bulk size and unwanted high torque ripple were unavoidable [14].

While dual stator design is configured with single constant magnetic rotor and two stator (DSPM-SR) design, outer and inner stator structure. The coils are typically wound around the stator teeth which deliberately results two sets of independent torque leading to a relative high of motor's torque density and flux linkages that were about doubly than the conventional design geometry [15, 16]. The investigation is then extended with design variations of slotted stator such as Double Stator Arc Permanent Magnet (DSPM-AP), Double Stator Double Pole (DSPM-DP), Double Stator with Interior Magnet (DSPM-IP), Double Stator with Cup Rotor (DSPM-CR) and DSPM-SR for optimum torque performance i.e. constant torque density and desirable efficiency [17]. Again, parasitic effects like high cogging torque and high torque ripple together with manufacturing constraints like complex in fabrication leading to high cost were not avoidable. Instead of cogging torque elimination, the PM motor topologies as in Figure 2 are radial flux oriented. It should be noted that the magnets are still can be magnetized in radial or parallel direction. For the same stator configuration as shown in Figure 3 [18], its rotor magnets can be surface mounted or buried (interior mounted). Although the Interior Permanent Magnet (IPM) motor is superior than the Surface Mounted Permanent Magnet (SPM) motor due to L_q and L_d characteristic for flux-weakening control, the SPM motor is still a competitive candidate to replace the IPM motor because of less complexity in fabrication process.

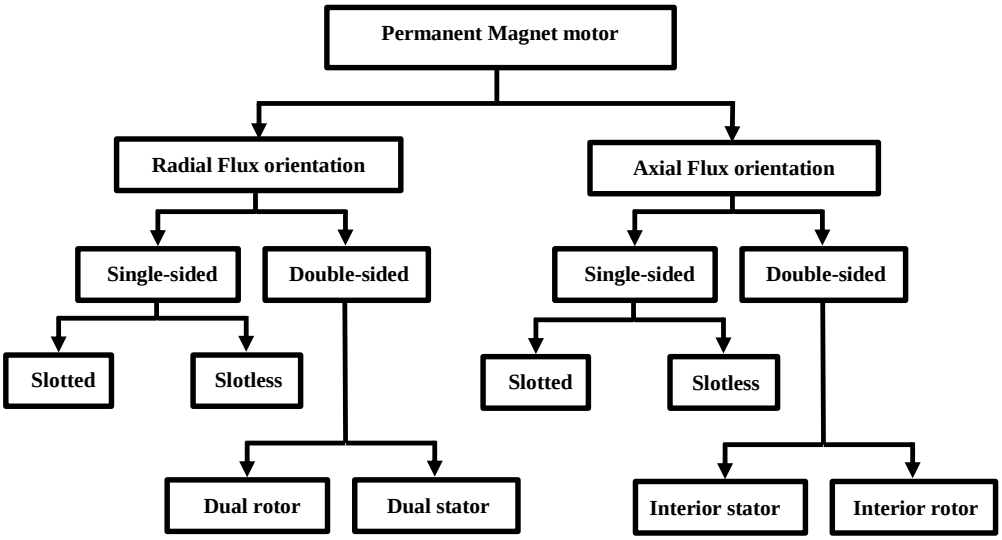

Figure 1. An overview of PM motor topologies

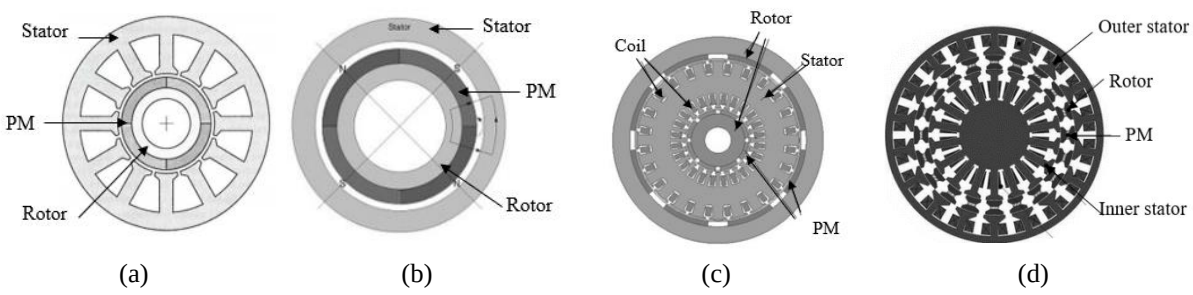

Figure 2. Radial flux orientation PM motors [11], (a) slotted (single-sided), (b) slotless (single-sided), (c) double rotor, (d) double stator

Figure 3. Type of permanent magnet rotor topologies [18], (a) surface mounted, (b) interior mounted

Instead of conventional slotted radial flux SPM motor designs, the axial flux oriented motors which geometry is a pancake looked alike is an alternative. For axial flux designs with slotted stator, the motors are advantageous in term of shorter stack length, achieveable high torque density and high efficiency as compared to the slotted, radial flux configuration [19-22]. In addition, these motor topologies offer better ventilation and heat removal [23].Similar to conventional flux topologies, AFPM motors also can be constructed in single sided or double sided, and with or without slots. For slotted axial flux configuration, the single-sided structure results simple geometry and cheaper but potentially having poor performance i.e. low torque density, low efficiency, high cogging torque and unbalanced magnetic force as compared to the other axial flux topologies [24]. While for non-slotted type, high power-to-weight ratio, low inductance leakages, minimum cogging torque and low vibration are possibly achieved [25].

Better torque performance can be achieved by having dual-sided configuration such as one-stator two-rotor (TORUS) and two-stator-one-rotor (AFIR) designs. In many cases, these topologies result high-torque density, balanced magnetic force and high power density instead of single-sided type. In [26], the comparison of TORUS and AFIR motor with slotted and non-slotted configurations were investigated. The slotted TORUS design resulted high torque density with a relative small electrical loading. While the AFIR motors, a relative low current density for a similar amount of electrical loading is obtained. For non-slotted configuration, both designs would have minimum cogging torque and low torque ripple than slotted type [27]. However, complex design, severe torque pulsation and low torque density in various on-load situations were inherited compared to the conventional motors design [25].

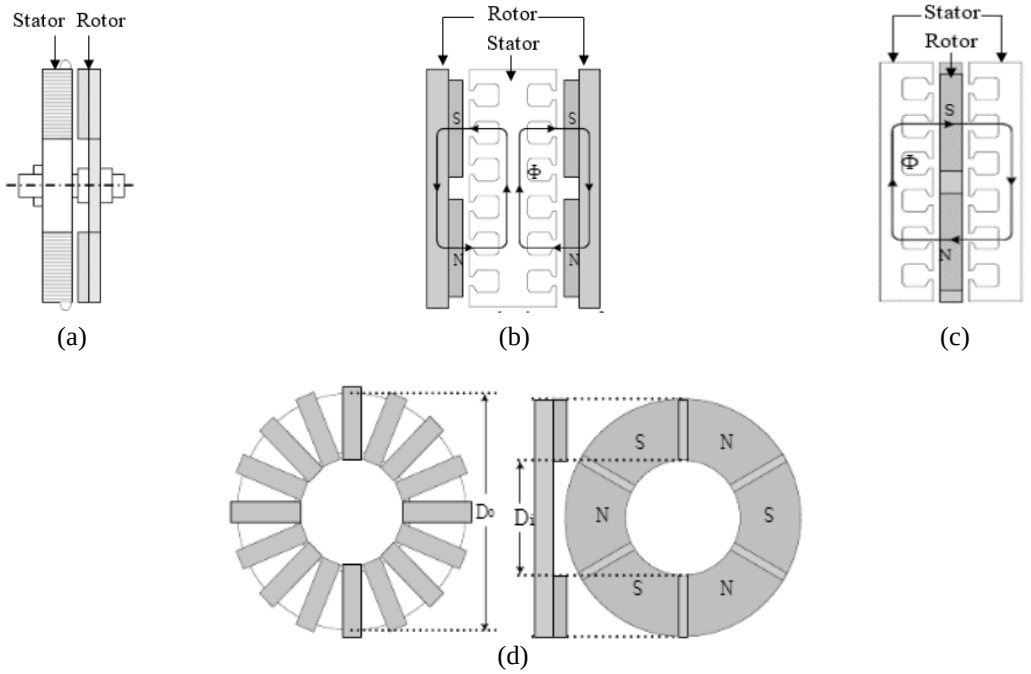

Figure 4. Axial flux orientation PM motors [24], (a) Single-sided, (b) Interior stator (double-sided), (c) Interior rotor (double-sided), d) Slotless vs slotted

In this article, further investigation on the developed prototype in [28, 29] equipped with asymmetric stator design is carried out to ensure significant reduction of overall motor weight is successfully achieved while maintaining desired torque performance. As the initial approach was taken by by removing partial stator magnetic iron path which inherently results a hemicycle stator equipped with a set of an asymmetric disposition of phase coils, a little modification at both ends of the hemicycle stator is introduced. The investigation is carried out using 2D-Finite Element Analysis in which non-linear saturation condition is included.

2. ANALYSIS OF HEMICYCLE STATOR DESIGN

A PM motor in which design is configured with a hemicycle stator is basically derived from a slot number/pole number combination of Ns =2p±2 [29]. The configuration results a symmetric disposition of coils for each phase and proved by the balanced winding mmf vectors among phases. Thus, by removing partial stator magnetic iron path, a balanced set of the mmf vectors is still visible. However, this situation will not be occurred for PM motors in which Ns =2p±1. Table 1 tabulates parametric specifications over slight change on geometry of hemicycle stator. The motors are designed to run at a rated speed of 100 rpm while the excitation current depends on the back-emf profiles i.e. 10A for conventional topology while 3A for hemicycle stator topology. Silicon steel and Neodynium Iron Boron (NdFeB) are the soft and hard magnetic materials used for modeling and analysis. Table 2 compares a few possible combinations of PM motors that can be converted into hemicycle motor configuration. It is shown that the winding factors between the two design topologies are remain unchanged. It should be noted that the removal of partial stator iron magnetic paths in the early stage resulted poor motor performance.

Table 1. Parametric specification over various stator design

Parameter	Specifications			
Model configuration	Design 1	Design 1 (optimized)	Design 2	Design 3
Outer stator radius (mm)	60			
Inner stator radius (mm)	36			
Split ratio	0.6			
Tooth body width (mm)	13.1	11.1	11.1	11.1
Coil turns per phase	104	136	104	136
Arc length (mm)	188.52	188.52	188.52	~204.23
Length covered between arc ends (mm)	0	0	5mm inward	5mm outward
Stator back iron depth (mm)	6.7			
Slot depth (mm)	13			
Stack length (mm)	20			
Magnet thickness (mm)	5			
Airgap thickness (mm)	1			
Slot opening (mm)	1.1			
Tooth tip height (mm)	3.3			
Operating mode	DC			

Table 2. Potential slot numbers for hemicycle configuration when 2p =10

Pole number (2p)	Conventional		Hemicycle	
	Slot number	Winding factor	Slot number	Winding factor
10	6	0.50	3	0.5
	9	0.94	-	-
	12	0.96	6	0.96
	15	0.86	-	-
	18	0.74	9	0.74

From the previuos investigation [29], an optimum width of stator teeth and suitable number of coil turns per phase with respect to the slot area played important roles in enuring optimum electromagnetic performance. In this stage, further investigation is carried out by introducing additional modification on the magnetic iron path at both ends of stator arc; i) introducing additional stator tooth of 5mm thick, which space taken over the area of both end slots (*Design 2*), ii) introducing extended arc length of 5mm length (~204.23 mm in total instead of 188.52) beyond the 180° angle of hemicycle shape (*Design 3*). Figure 5

visualizes these modifications. The main idea to impose this additional magnetic iron path is to ensure all magnetic fluxes dvelope a closed loop circuit along the satator and rotor which in principle can exhibit optimum motor performance via acceptable back-emf and torque waveforms.

For Design 2, the additional stator tooth within 180° arc may limit the slot area and number of coil turns which inherently affect desired electric loading, While, Design 3 may exhibit suitable magnetic flux distribution and better output performance for a similar number of coil turns. Figure 6 compares the winding arrangements implemented between the conventional dan hemicycle design topologies. For extended works, the Design 3 becomes a main subject as the influence of modification on both stator arc ends is investigated.

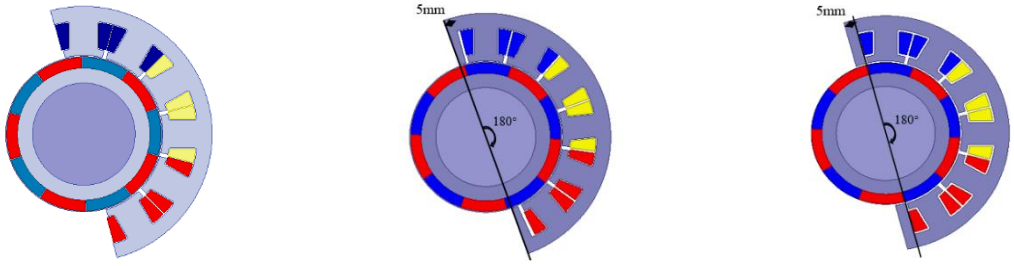

(a) (b) (c)

Figure 5. Geometry layouts, (a) Design 1 (180°, arc length 188.52 mm), (b) Design 2 (180°, arc length 188.52mm), (c) Design 3 (> 180°, arc length ~204.23mm)

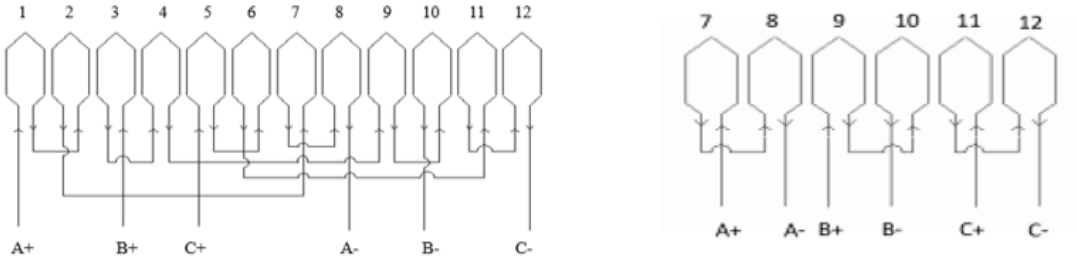

(a) (b)

Figure 6. Winding layouts, (a) conventional (12-slot), (b) Design 1, 2 and 3 (6-slot)

2.1. Weight of proposed PM motor design

The weight of standard motor design is formulated as follows:

$$W_s = \left\{ \left[\frac{\pi d_{so}^{\ 2}}{4} - \frac{\pi d_{si}^{\ 2}}{4} - A_s \right] \times L_a \right\} \times \rho_{ss} \quad (1)$$

$$W_c = \left\{ \left\{ \pi r_c^{\ 2} \times \left[2(S_{tbw} + L_a) \times N_t \right] \right\} \times N_s \right\} \times \rho_c \quad (2)$$

$$W_m = \left\{ \frac{P_p}{2\pi} \left\{ \left[\frac{\pi d_{mo}^{\ 2}}{4} - \frac{\pi d_{mi}^{\ 2}}{4} \right] \times L_a \right\} \times N_p \right\} \times \rho_m \quad (3)$$

where W_s, W_c, W_m are the weight of stator, copper winding and permanent magnet respectively. While d_{so}, d_{si}, A_s , L_a , r_c , S_{tbw} , N_t , N_s , N_p , P_p , d_{mo} , d_{mi} , are the outer stator diameter, inner stator diameter, slot area, axial length, radius of copper coil, tooth body width, number of turns of copper coil, slot number, pole number, pole-pitch, outer rotor magnet, and inner rotor magnet respectively. For the mass densities, p_{ss} , p_c , p_m are the mass density of silicon steel [7600 kg/m^3], mass density of copper [8960 kg/ m^3] and mass density of NdFeB permanent magnet [7400 kg/ m^3] respectively. For the hemicycle motor, the weight of stator body, copper winding and permanent magnet are mathematically derived as follows:

$$W_{sh} = \left\{ \frac{180}{360} \left[\frac{\pi d_{so}^{\ 2}}{4} - \frac{\pi d_{si}^{\ 2}}{4} - A_s \right] \times L_a \right\} \times \rho_{ss} \quad (4)$$

$$W_{hc} = \left\{ \left\{ \pi r_c^{\ 2} \times \left[2\left(S_{tbw} + L_a \right) \times N_t \right] \right\} \times N_s \right\} \times \rho_c \quad (5)$$

$$W_{mh} = \left\{ \frac{P_p}{2\pi} \left\{ \left[\frac{\pi d_{mo}^{\ 2}}{4} - \frac{\pi d_{mi}^{\ 2}}{4} \right] \times L_a \right\} \times N_p \right\} \times \rho_m \quad (6)$$

where W_{sh}, W_{ch}, W_{mh} are the total weight of stator, copper windings and permanent magnets respectively.Finally, the formulated weights are summed up as:

$$W_T = W_s + W_c + W_m \quad (7)$$

Table 3 compares the individual weight fractions of each motor design involved. The fractions of these weights are stator body, copper winding and permanent magnet. It is shown that theoretically the weights of standard motor design and all hemicycle designs are 1.368 kg and 0.68kg respectively, and results 44% reduction significantly.

Table 3. Breakdown Weight in propose motors design

Materials	Standard motor	Design 1	Design 2	Design 3
Stator body (kg)	1.032	0.518	0.519	0.556
Copper windings (kg)	0.256	0.098	0.098	0.128
Permanent magnets (kg)	0.08	0.08	0.08	0.08
Total weight (kg)	1.368	0.696	0.697	0.764

3. RESULTS AND ANALYSIS

3.1. Modification on hemicycle stator ends

Figure 7 compares the flux-lines of all designs at no-load condition. It can be seen that the fluxes in Design 2 and 3 are highly concentrated than in the Design 1. In other way, the little modification at both ends of the hemicycle stator results new route for the fluxes to complete as closed magnetic circuit. This phenomenon would help the motors to have better electromagnetic characteristics such as flux-linkages and back-emfs.

The back-emf's characteristics of all designs are compared in Figures 8(a)-(b). Obviously, the Design 1 has shown a 33% increament of back-emf from 3V to 4V together with enlargement shape which later becomes Design 3. However, no significant change of phase back-emf exists in Design 2 as the slot area adjacent to the 5mm inward tooth is squeezed leading to a highly potential of quick saturation condition. The harmonics contents in each back-emf can be compared in Figure 8(b). The rise of higher multiple order harmonic (3^{rd}, 5^{th}, 7^{th} ,etc.) indicates dented peaks in all back-emfs. Interestingly in Figure 8(c), the flux-linkages in all design are relatively sinusoidal which opposes their respective back-emf's shapes. The peak flux-linkage in Design 1 is 0.06 Wb and rose up to 33% in Design 3. While Design 2 results no significant change of flux linkage due to smaller slot area and less number of copper turns.

Figure 9 compares the static torque in all designs. Again, the Design 3 results better torque performance in term of torque average torque and torque ripple. The torque average increases around 23%, from 4.8 Nm in Design 1 to 5.9 Nm and the torque ripple reduces significantly around 50%. Meanwhile, severe torque performance exists in Design 2 where its respective torque average and torque ripple contras to the one obtained by Design 3. It should be noted that the torque is calculated in static condition in which six-step commutation for 1 electrical cycle is implemented as theorectically applied in convetional PM motors. It also should be taken into consideration that an intelligent switching scheme must be carefully designed to encounter the unconventional torque waveform.

In term of cogging torque, the Design 1 and its optimized model (Design 1 optimized) result maximum peak of 0.96 Nm as shown in Figure 10. However, the peak reduces when Design 2 and Design 3 are introduced where their individual percentage of reductions are 9.4% and 34% respectively. An obvious finding is obtained in Design 3 where there are reductions of maximum peak in alternate cycles as well as an increase in cogging cycles. This phenomenon exists due to due to the additional 5mm thick tooth body at both ends of hemicycle stator in which high magnetic permeance is achieved.

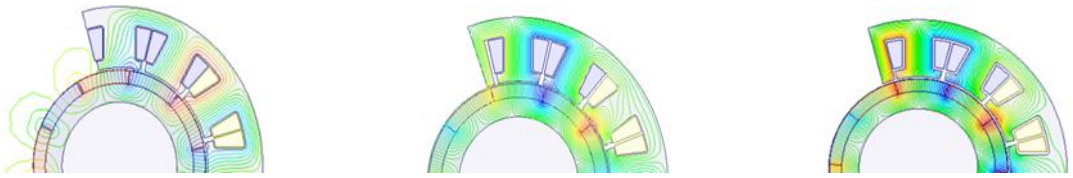

(a) (b) (c)

Figure 7. Flux contours at no-load condition, (a) Design 1, (b) Design 2, (c) Design 3

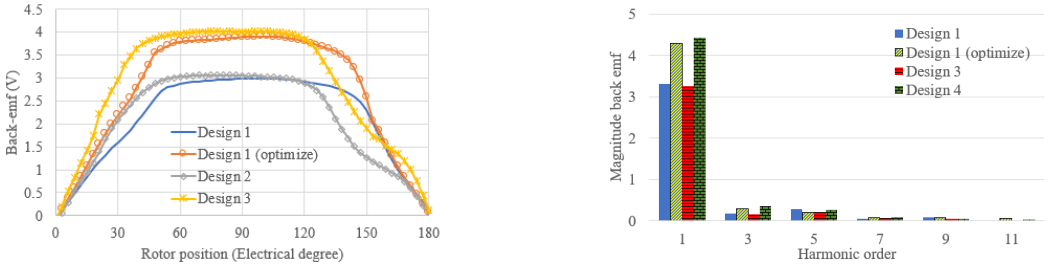

(a) (b)

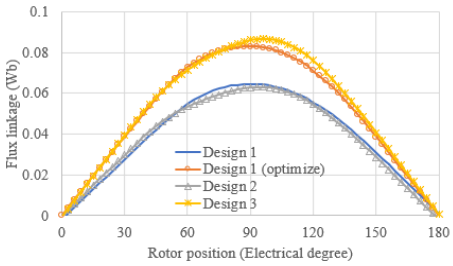

(c)

Figure 8. Back-emfs and flux-linkages; a) Phase back-emfs, b) harmonics in phase back-emfs, c) flux linkage

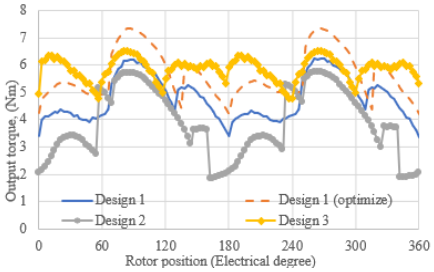

Figure 9. Static electromagnetic torque

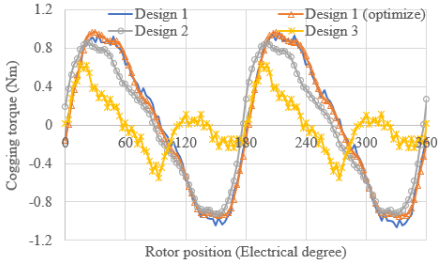

Figure 10. Cogging torque

3.2. Influence of tooth thickness at both ends of hemicycle stator

From the preceding section, the Design 3 is the best model for the hemicycle stator design. The question arises after the whole discussion is on the selection of 5mm thickness which results in extended stator arc length of ~204.23 mm instead of 188.52 mm. In this section, a detailed analysis of the influence of additional tooth with 5mm thickness on both stator ends is broken down to its effect on phase back-emf, flux-linkage, static torque and cogging torque respectively. Figure 11(a) compares the phase back-emf over specific ranges of end tooth thickness. There is a slight increase of peak back-emf when 4 mm is included, and the waveform remains unchanged when the thickness is varied up to 6 mm. A similar trend is duplicated by the flux-linkages as shown in Figure 11(b). In term of static torque as shown in Figure 11(c), the torque average and torque ripple in all designs over specific tooth thicknes are relatively constant. However, 5 mm thicknes would be a good choice as it compromises between achieveable torque average and a slight lower torque ripple. In term of cogging torque as shown in Figure 11(d), thicker tooth results smaller cogging torque and introduce higher cogging cycles. This would be good for torque production as it lessen the parasitic effect on the torque ripple and vibration as well. All information related to the above analysis is tabulated in Table 4.

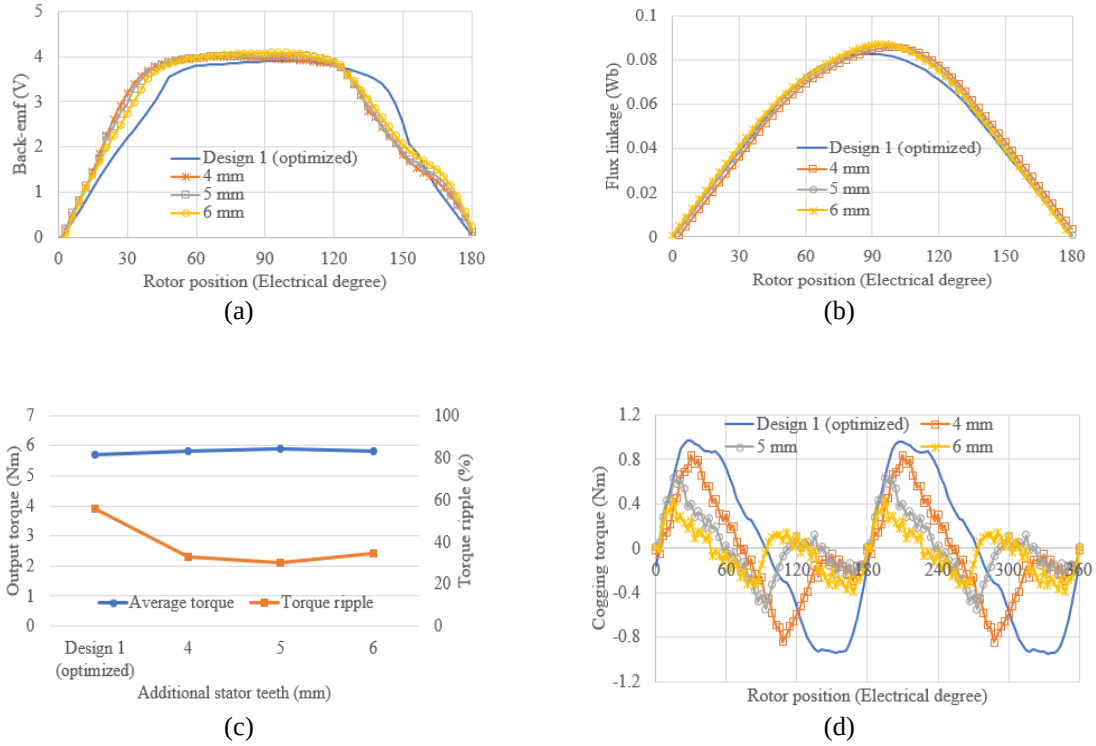

Figure 11. Electromagnetic performance over variation additional stator tooth, (a) Phase back-emf, (b) Flux-linkage, (c) Static torque (d) Cogging torque

Table 4. Overall electromagnetic characteristic in the proposed motor design

	Design / Modification	Configuration	Peak back-emf (V)	Flux-linkage (Wb)	Torque Average (Nm)	Torque ripple (%)	Cogging torque (Nm)
1	Hemicycle stator design	Design 1	3.0	0.06	4.8	60.0	0.96
		Design 1 (optimized)	3.9	0.08	5.7	55.6	0.96
		Design 2	3.0	0.06	3.9	99.8	0.87
		Design 3	4.0	0.09	5.9	30.0	0.63
2	Additional stator tooth in Design 3 (mm)	0	3.9	0.08	5.7	55.6	0.96
		4	4.0	0.09	5.8	32.8	0.84
		5	4.0	0.09	5.9	30.0	0.63
		6	4.0	0.09	5.8	34.6	0.44

4. CONCLUSION

It can be concluded that a PM motor equipped with a hemicycle stator theoretically can operate as a regular conventional PM motor. Its main advantage is the reduction of total weight reduction as derived analytically. The analytical model used to represent the overall weight of hemicycle motor is then compared and verified with with a conventional PM motor design. It is also found that a little modification on magnetic iron path on both ends of hemicycle stator results an optimum performance of hemicyle PM motor. It is believed that the optimum performance is obtained when the magnetic permeance in a closed magnetic circuit is improved.

ACKNOWLEDGEMENTS

The authors would like to thank Universiti Teknikal Malaysia Melaka (UTeM) for providing the research fund of UTeM Zamalah Scheme.

REFERENCES

[1] Emadi, A., "Energy Efficient Electric Motors". 3rd ed. 2005, New York: Marcel Dekker.
[2] Manoj et al, "FEA of a High Efficiency Brushless DC Motor Design," *International Journal of Applied Engineering Research*, vol. 12, no. 1, pp. 11417-11423, 2017.
[3] Shivraj and Archana, "Mathematical Modelling and Simulation of Three Phase BLDC Motor Using MATLAB," *International Journal of Advance in Engineering & Technology*, 2014; 1426 – 1433.
[4] Shirish and Jain, "Modelling and Simulation of Three Phase BLDC Motor for Electric Braking Using MATLAB/SIMULINK," *International Journal of Electrical, Electronics And Data Communication*, vol. 5, no. 7, pp. 48-53, 2017.
[5] Yang M. et al, "A Cost-Effective Method of Electric Brake with Energy Regeneration for Electric Vehicle," *IEEE Transaction on Industrial Electronics*, vol. 56, no. 6, pp. 2203-2212, 2009.
[6] Talebi et. al., "An Improved Method to Control the Speed of PM-BLDC Motors," *6th International Power Electronics Drive Systems and Technologies Conference*, IEEE Publisher, 3-4 February 2015.
[7] Seo, J. M. et al, "Design of Axial Flux Permanent Magnet Brushless DC Motor for Robot Joint Module," *The 2010 International Power Electronics Conference*, pp. 1336-1340, 2010.
[8] Zhou L., Bai S., and Hansen M. R., "Design Optimization on The Drive Train of a Light-weight Robotic Arm," *Mechatronic*s, vol. 21, issue 3, pp. 560–569, 2011.
[9] Amit N. P. et al, "Influence of Difference Type of Stator Slots on Torque Profile of Surface Mounted Pm Motors," *International Journal of Computer Applications in Engineering Sciences*, vol. 5, no. 2, pp. 40-42, 2014.
[10] Arora A. S. and Gurmeet S., "Review of Design and Performance of Permanent Magnet Synchronous Motor," *Proceeding of The IRES 6th International Conference*, Melbourne, Australia, pp. 107 – 115, 2015.
[11] Ilka R. et. al., "Design of Slotless BLDC Motor for Elimination Cogging Torque," *Journal of World's Electrical Engineering and Technology*, vol. 3, no. 2, pp. 67-73, 2014.
[12] Ronghai Q. and Thomas A. L., "Dual-Rotor, Radial-Flux, Toroidally Wound, Permanent Magnet Machines," *IEEE Transactions on Industry Application*, vol. 39, no. 6, pp. 1665-1673, 2003.
[13] Song S. et. al., "Design and Simulation of Dual Rotor Permanent Magnet Brushless DC Motor," *17th International Conference on Electrical Machines and Systems*, IEEE Publisher, pp. 1591-1595., 2014.
[14] Pisek P. et. al., "Performance Comparison of Double and Single Rotor Permanent Magnet Machines," *Przeglad Elektrotechniezny*, vol. 87, no 3, pp. 133-136, 2011.
[15] Swivedi A. and Srivastava R. K., "Analysis of Dual Stator PM Brushless DC Motor," *IOSR Journal of Electrical and Electronics Engineering*, vol. 1, no. 2, pp. 51-56, 2012.
[16] Firdaus R. N. et. al., "Modelling of torque and speed characteristics of double stator slotted rotor brushless DC motor," *IET Electric Power Applications*, vol. 12, no. 1, pp. 106-113, 2018.
[17] Firdaus R. N. et. al., "Torque Constant Density in Different Type of Double Stator Permanent Magnet Brushless DC Motor," *Progress in Electromagnetic Research M*, vol. 66, pp. 127-142, 2018.
[18] J. R. Hendershot & T. J. Miller, "Design of Brushless Permanent Magnet Machines" in Motor Design Books, USA: Florida, 2010.
[19] Cavagnino A. et al, "A comparison between the Axial Flux and the Radial Flux Structures for PM synchronous Motors," *IEEE Transactions on Industry Applications*, vol. 38, no. 6, pp. 1517-1524, 2002.
[20] Seo, J. M. et al, "Design of Axial Flux Permanent Magnet Brushless DC Motor for Robot Joint Module," *The 2010 International Power Electronics Conference*, Sapporo, pp. 1336-1340, 2010.
[21] Guo B. and Huang Y., "A fast-analytic model of axial flux permanent magnet machines with static/dynamic axis eccentricity," *Journal Magnetic*, vol. 21, pp. 554-560, 2016.
[22] Bouaziz O., et. al., "Performance analysis of radial and axial flux PMSM based on 3D FEM modelling," *Turkish Journal of Electrical Engineering and Computer Sciences*, vol. 26, no. 3, pp. 1587-1598, 2018.
[23] Mahmoudi A., Rahim N. A., and Hew W. P., "An analytical complementary FEA tool for optimizing of axial-flux permanent magnet machines," *International Journal of Applied Electromagnetics Machines*, vol. 37, no. 1, pp. 19-34, 2011.

[24] Aydin M. et. al., "Axial Flux Permanent Magnet Disc Machines: A review," Wisconsin Power Electronics Research Centre, September 2004.
[25] Jacek F. G., Wang R. and Maarten J. K., "Axial Flux Permanent Magnet Brushless Machines," 2nd Edition. Springer, 2008.
[26] Mahmoudi A., Ping H.W. and Rahim N.A., "A comparison between the TORUS and AFIR axial-flux PM machine using finite element analysis," *Proceeding IEEE International Electrical Machines and Drives Conference*-IEMDC 2011, pp. 242-247, 2011.
[27] Mahmoudi A., Rahim N. A. and Hew W. P., "TORUS and AFIR axial-flux permanent-magnet machines: A comparison via finite element analysis," *International Review on Modelling and Simulations*, vol. 4, no. 2, pp. 624-631, 2011.
[28] M. Luqman, Kwang T. C. and Auzani J., "Design and Analysis of PM motor with Semi-circle Stator Design using 2D-Finite Element Analysis," *Indonesian Journal of Electrical Engineering and Computer Science*, vol. 13, no. 1, pp. 427-436, 2019.
[29] Kwang T. C., Luqman M. and Auzani Jidin, "Torque improvement of PM motor with semi-cycle stator design using 2D-finite element analysis," *International Journal of Electrical and Computer Engneering*, vol. 9, no. 6, pp. 5060-5067, 2019.

BIOGRAPHIES OF AUTHORS

Tan Cheng Kwang was born in Kelantan, Malaysia in 1994 and received the B. Eng degree in Electrical from Universiti Teknikal Malaysia Melaka Malaysia (UTeM), Melaka, Malayisa in 2018. He is currently pursuing his Master of Science at Universiti Teknikal Malaysia Melaka, Malaysia.

Mohd Luqman Mohd Jamil received B.Eng. degree from the Universiti Teknologi MARA, Shah Alam, Malaysia, in 2000, M.Sc. degree from Univeristy of Newcastle upon Tyne, U.K., in 2003, and Ph.D. degree from The University of Sheffield, Sheffield, U.K., in 2011, all in electrical engineering. He is currently an academician in Faculty of Electrical Engineering, University Teknikal Malaysia Melaka, Melaka, Malaysia. He is also an active researcher in Power Electronics and Drives Research Group (PEDG) that established under the same faculty. His research interests include the design, control and analysis of permanent-magnet machines.

Auzani Jidin received his B. Eng, M. Eng. And Ph.D, in Power Electronics and Drives from Universiti Teknologi Malaysia (UTM), Johor, Malaysia in 2002, 2004 and 2011 respectively. He is an academician in Department of Power Electronics and Drives, Faculty of Electrical Engineering, Universiti Teknikal Malaysia Melaka Malaysia. His research interest includes the field of power electronics, motor drives systems, field programble gate arrays and digital signal processing applications.